Journal of Membrane Science and Research 4 (2018) 85-92

Journal of Membrane Science & Research

journal homepage: www.msrjournal.com

Research Paper

# Insight of Interactions during Uptake and Permeation in Nafion Ionomer Membrane

Jayshree Ramkumar [1,*], S. Chandramouleeswaran [1], M. Basu [2], K.V. Vrinda Devi [3]

[1] Analytical Chemistry Division, Bhabha Atomic Research Centre, Mumbai-85, India
[2] Chemistry Division, Bhabha Atomic Research Centre, Mumbai-85, India
[3] Radiometallurgy Division, Bhabha Atomic Research Centre, Mumbai-85, India

## Article info

Received 2017-09-12
Revised 2018-01-16
Accepted 2018-01-16
Available online 2018-01-16

## Keywords

Nafion, pre-treatment
Spectral changes
Thermal properties
Optical images
Dye permeation

## Graphical abstract

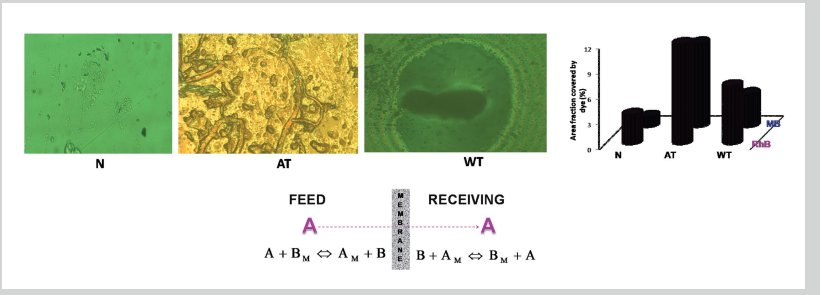


## Highlights

- Pretreatment with boiling acid or water changes the hydration of membrane
- The formation of water clusters identified by changes in the UV Vis spectra.
- Thermal studies also indicate the probable change in structure due to pretreatment procedure.
- Change in permeation properties of membrane as a result of pretreatment procedure.
- The nature of dye within the membrane also affects the thermal properties.

## Abstract

The effect of pre-treatment on the permeation property of the Nafion ionomer membrane has been evaluated. The membranes were subjected to different pre-treatment procedures, viz treated with acid at room temperature, boiling with acid or boiling with water followed by cold acid. Different characterization techniques were used to understand the changes. From UV-Visible spectra, it was possible to identify the presence of water clusters and this was found to be maximum when the membrane was boiled with acid. Thermal analysis of the membranes also reflected the changes in structure due to pre-treatment. The characterizations of dye loaded membranes were also carried out. Image analysis reflected the changes in structure due to pre-treatment. The spectrophotometric and thermal studies of the dye loaded membranes carried out showed that the two dyes interacted differently with Nafion. The permeation of dyes through Nafion showed that values of permeability and diffusion coefficients were also dependent on the nature of both the dye and pre-treatment procedure.



## 1. Introduction

Nafion, a perfluorosulphonate ionomer (PFSI) with polyfluoroethylene backbone and regularly spaced perfluorvinyl ether pendant side chains terminated by a sulphonate ionic group containing 10-mol% ionic content has unique properties of ionomers due to the formation of ionic clusters dispersed in the polymer backbone [1,2]. A study of the transport process in membranes is useful for both separation and process understanding [3-5]. The property of perm selectivity of ion exchange membranes is dependent on various external parameters [6-9]. For ion exchange membranes, the diffusion coefficient is dependent on selectivity coefficient indicating that the initial stage of permeation is governed by the ion exchange process [10]. Shelf-life has a very strong effect on the ion exchange and water sorption properties of membranes [11, 12]. The role of modifiers within the membrane and the effect on permeation across the membrane is of sustained interest [13-15].

Ion exchange membranes are extensively used for different separations. However, the studies on the structural aspects are also of great interest. Earlier studies showed the use of different techniques to probe the cluster model proposed for Nafion structure [1, 16-19]. These models showed that the ionic clusters present in the membrane swell when the membrane is hydrated. The structural studies give an idea of the mechanism of water transport through Nafion membranes, which makes it very useful in fuel cell applications.

The effects of different experimental conditions like pre-treatment of Nafion membrane and external conditions of pH and presence of complexing agents were found to affect the sorption or permeation behaviour for the Nafion membrane [6-12, 15]. The effect of the pre-treatment procedure on the sorption/permeation property of Nafion could be attributed to the changes occurring within the Nafion structure. The external solution conditions like pH or presence of different complexing agents also affect the sorption / permeation. This could be due to the fact that the complexing agents convert metal ions into anionic complexes and the property of perm selectivity is found to have a crucial role. Based on these findings, it was thought meaningful to study the permeation of cationic dyes through Nafion, since an

* Corresponding author at: Phone: +91 22 25592224
E-mail address: jrk@barc.gov.in (J. Ramkumar)

DOI: 10.22079/JMSR.2018.71696.1159

attempt of this nature has not been carried out earlier. In the present work, permeation of cationic dyes like Rhodamine B (RhB) and methylene blue (MB) have been studied using Nafion membranes pre-treated in different ways. In order to understand the mechanism of the sorption, the dye incorporated membranes were characterized using different techniques like spectrophotometry and image analysis to get an insight into the changes occurring during pre-treatment.

## 2. Experimental

### *2.1. Materials*

Nafion 117 obtained from DuPont was used for all studies. The membrane was cut into small pieces of 1cm × 1cm for the uptake studies. The permeation studies were carried out using circular pieces of 35 mm diameter. The membrane pieces were pretreated differently and stored in distilled water prior to their use. The aqueous dye solutions of Rhodamine B and Methylene blue were prepared from the dyes obtained from Merck without any purification.

### *2.2. Instrumentation*

Thermal gravimetric analysis (TGA) was performed using a Setaram equipment (Setsys Evolution 1750) at a heating rate of 10°C/min under flowing Ar atmosphere. The sample size was within 4-5 mg. The images for analysis were acquired using an optical microscope (LEICA-DM ILM) coupled with digital camera. Interpretation of data was carried out using an image analysis software (Metal power image analyser version 3.0.0.9 by Metal Power India (Pvt. Ltd).). Spectrophotometric measurements were carried out using JASCO V-650 Series double beam spectrophotometer in the wavelength range of 190-900 nm.

### *2.3. Procedure*

Pre-treatment of the Nafion membranes were carried out in three different manners (i) immersion of as received membrane in cold 2 M HCl for 2 h, removed and washed well with distilled water to give sample labelled **N,** (ii) membrane pieces refluxed with 1:1 $HNO_3$ for 1 h and then boiled with distilled water (~60 °C) for 1h and samples labelled **AT**, (iii) membrane pieces boiled with distilled water for 2 h and then immersed in cold 2 M HCl for 2h and sample labelled **WT**.

The experimental setup for sorption and permeation experiments is shown in Figure 1. Both water and dye sorption studies were carried out in batch mode using the experimental setup shown in Figure 1a. For water sorption studies, the accurately weighed amount of Nafion membrane (pre-treated in different ways) was soaked in 200 mL of deionised water at room temperature. The increase in weight was measured as a function of time until the moisture content attained an equilibrium value (incremental change of sample mass < 0.001 g for 1 h). The water sorption studies were carried out in triplicate. The dye loaded membrane samples were prepared by equilibrating 0.25 g of Nafion membrane (pre-treated differently) with 25ml of dye solution for 6 h.

The permeation experiments were carried out in a specially designed U type cell consisting of two flat ground ends of standard flanged joints FG 15 (Quick Fit, UK) connected to a bent glass tube (Figure 1b). The circular pieces of the clean membrane (pre-treated differently) were placed tightly between the clamps and the system is leak proof with the two compartments viz Feed (F) and Receiving (R) on either side of the membranes. The feed compartment contained 20mL of dye solution of known concentration maintained at a particular pH while receiving 20 mL of 0.01M acid. The solutions in both the compartments were continuously stirred using magnetic stirrers to reduce concentration polarization. The dye concentration in the receiving phase was monitored by measuring the absorbance at 554 and 662 nm for Rhodamine B and Methylene blue, respectively.

## 3. Results and discussion

Permeation studies were carried out with the Nafion membrane pre-treated differently (N, AT, WT) prior to use. Our earlier studies showed that the pre-treatment procedure [10-12] has an effect on the sorption and permeation properties. Thus, it became very interesting to see if we can understand the changes occurring using various characterization techniques.

### *3.1. Characterization Studies of pre-treated Nafion membranes*

Water sorption analysis was carried out using Peleg's model [20], which is normally used for food products like chickpeas, etc. The major advantage of the Peleg model is that the analysis can be carried out using short time experimental data unlike the Darcy Watt Analysis reported earlier [11,12]. Another important aspect of the Peleg model is that there is no criterion set for the selection of the last data. However, certain researchers strongly felt that selection criterion was needed as the data selected could affect the constants obtained from the model. The linearized form of the Peleg model is given by Eq.1, wherein M is moisture content (%) at time t, $M_0$ is initial moisture content (%), $K_1$ is the Peleg rate constant ($h\%^{-1}$), and $K_2$ is the Peleg capacity constant ($\%^{-1}$). The increase in mass (+ in Eq.1) denotes absorption while decrease in mass (- in Eq.1) denotes the desorption reaction. The rate of sorption R is given by Eq.2.

$$M = M_0 \pm \frac{t}{K_1 + K_2 t} \quad (1)$$

$$R = \frac{K_1}{(K_1 + K_2 t)^2} \quad (2)$$

$$R_0 = \frac{1}{K_1} \quad (3)$$

The Peleg rate constant $K_1$ is related to sorption rate at the beginning ($R_0$), R at $t = t_0$ as given by Eq.3 and gives an idea of mass transfer, while the Peleg coefficient constant $K_2$ is related to maximum possible moisture content at $t = \infty$.

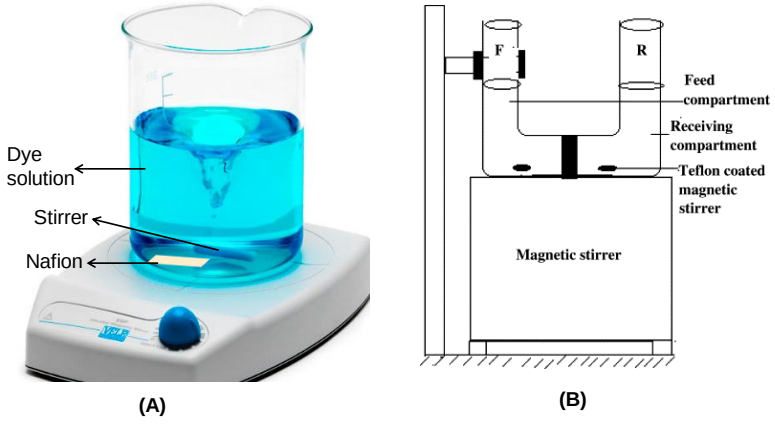


**Fig. 1.** Experimental setup for (a) sorption and (b) permeation studies.

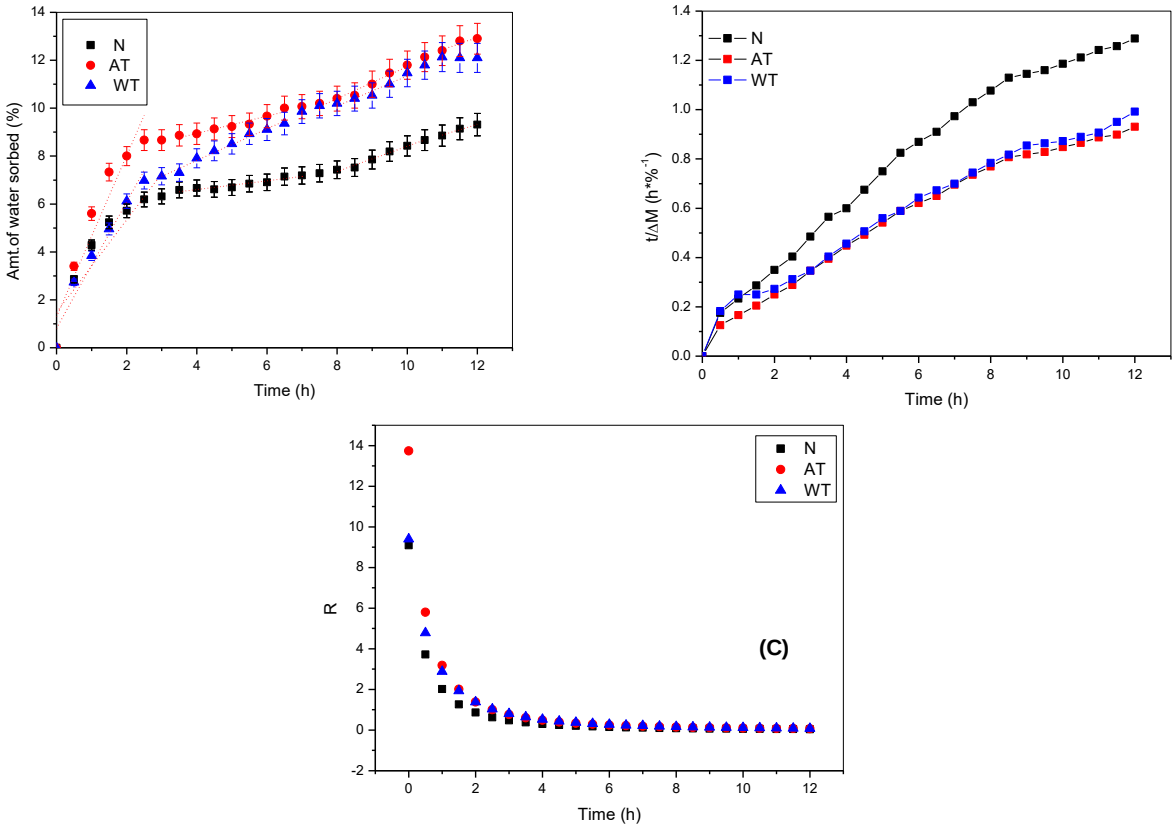


**Fig. 2.** Results of data modelling using Peleg's model.

The plot of amount of water sorbed (%) as a function time is given in Figure 2A. The data of water sorption is the average of triplicate studies with a 0.05% coefficient of variation. As there exists no concurrence on the protocol for data selection, the sorption curves (Figure 2A) could be divided into different linear segments. It is seen that for sample WT, there are only four linear segments whereas the plots of N and AT have five linear segments. The different parameters correlating to the plots are given in Table 1. From Figure 2A and Table 1, it is seen that pre-treatment has an effect on the maximum amount of water taken up ($M_e$). The calculation of Peleg's constants $K_1$ and $K_2$ are obtained from the linear plot of t/ΔM vs t (Figure 2B) and given in Table 1 (with a standard error value being less than 0.002). From Peleg's model, it is understood that the initial water sorption for the AT sample occurs at a higher rate (seen by lower $K_1$ value). The lower values of $K_2$ of AT and WT samples give an indication regarding the maximum water capacity (the lower the value of $K_2$ the higher the amount of water taken up). The plot of rate of sorption (R) versus time is given in Figure 2C. It is seen that AT has a high initial sorption rate and this is in accordance with the results shown in Figure 2B. With an increase in time, the sorption rate decreases.

Spectrophotometric analyses of the samples were carried out to see if pre-treatment induces some spectral changes. The results of the samples in $H^+$ form are shown in Figure 3.

**Table 1**
Data selection for fit of Peleg model and calculated values.

| Sample | $M_0$ | $M_e$ | Calculated values | | |
|---|---|---|---|---|---|
| | | | $K_1$ (h *%$^{-1}$) | $K_2$ (%$^{-1}$) | R (%*h$^{-1}$) |
| N | 1.0 | 8.5 | 0.1122 | 0.1237 | 9.09 |
| AT | 1.8 | 13.7 | 0.08133 | 0.0824 | 13.75 |
| WT | 1.4 | 10.6 | 0.12902 | 0.0885 | 9.94 |

It is to be noted that the spectra obtained for all three membranes have a broad maxima in the range of 250-280 with a small shoulder at 230 nm. The shoulder at 230 nm could be attributed to the C-F group, while the strong maxima could be due to the water clusters present in the Nafion. Before a comparison of the plots, it is to be noted that the spectra in the present study does not show a strong peak at 196 nm unlike that reported earlier [21], but in that work the authors have also seen a change in the spectra upon pre-treatment and variation of counter cation. In the present work, the spectra of N, AT and WT show a maxima at $\lambda_{max}$ of 266, 248 and 257 nm, respectively. All the spectra are associated with a shoulder at $\lambda_{max}$ ~ 220 nm. The shoulder at $\lambda_{max}$ ~ 220 nm could be due to the C-F groups or the diene structures, while the peaks near $\lambda_{max}$ ~ 260 nm could be attributed to the presence of the water clusters present in the Nafion membrane. It is observed that the peak at $\lambda_{max}$ ~ 220 nm is shifted to higher wavelengths while the peak at 266 nm is shifted to lower values upon pre-treatment. Thus, it is seen that pre-treatment increases the degree of hydration. Hydration leads to changes in morphology of the membrane, local aggregate structures and dissociation of the ions and this leads to reorganization of water clusters along the polymer geometry. These changes are reflected in the spectra of the pretreated Nafion membranes.

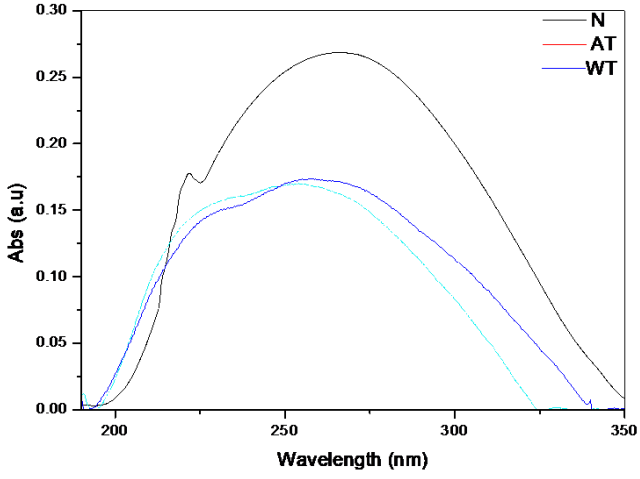


**Fig. 3.** UV Spectra of Nafion membranes (N, AT, WT).

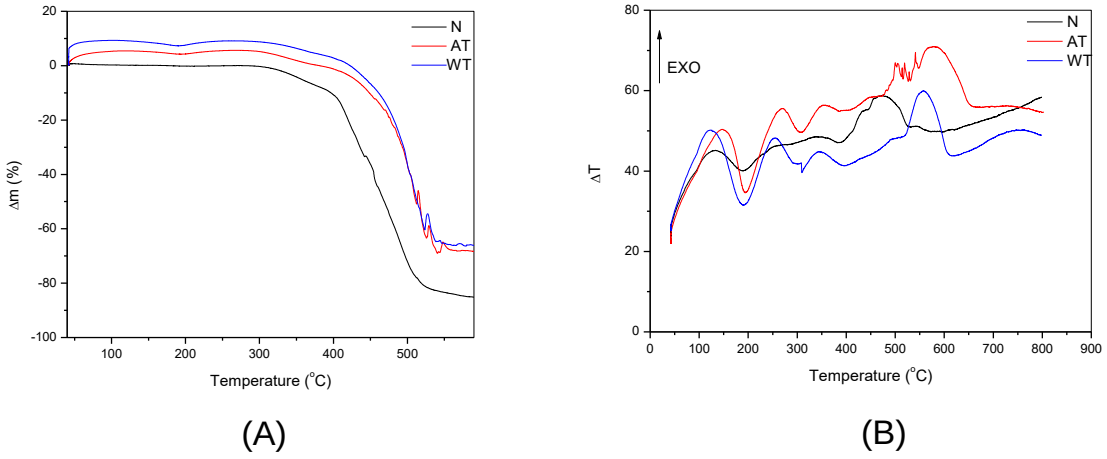


**Fig. 4.** Thermal data (A) TG and (B) DTA traces of Nafion-H pretreated differently.

**Table 2**
Data of thermal degradation of Nafion.

| Memb. | Step I (ºC) | Step 2 (ºC) | Step 3 (ºC) |
|---|---|---|---|
| | Desulphonation | side-chain decomposition | PTFE backbone decomposition |
| N | 303–401 | 401-441 | 441-510 |
| AT | 286-403 | 402-472 | 472-510 |
| WT | 294-415 | 415-479 | 479-530 |

Thermal studies were carried out to get an insight of the effect of pre-treatment on the membrane structure and the results are shown in Figure 4. Earlier studies [22] reported that the gases liberated in the temperature range of 25–355ºC were $H_2O$, $SO_2$ and $CO_2$ while in the range of 470–560 ºC HF, $SiF_4$ and $COF_2$ were liberated. The thermogram of Nafion –H form pretreated differently (Figure 4A) shows very interesting features. The weight losses measured for N, AT and WT are 79%, 73% and 71%, respectively.

The thermal degradation is seen to occur stepwise corresponding to desulfonation, side-chain and PTFE backbone decompositions and details are given in Table 2. The decomposition pattern of the Nafion is found to be affected by the pre-treatment procedure (Figure 4).

For all the membranes, it is seen that up to the temperature of onset of Step 1 (desulphonation), the weight change corresponding to the sorbed water loss is quite less. It is interesting to note that the onset and rate of desulphonation is greatly affected by pre-treatment. Step I starts at a lower temperature, but is spread over a larger temperature range for both AT and WT as compared to N. Another important feature that can be seen in the TG plots (Figure 4A) is that for AT and WT, and the PTFE backbone decomposition occurs at a higher temperature as compared to N. This could be attributed to increased rigidity of the backbone due to additional interactions between the protons within the clusters and F from the PTFE backbone leading to the formation of some kind of cyclic structures. This is due to the fact that pre-treatment results in the increase in the size of the clusters. All these changes are reflected in the difference in thermal behaviour of the Nafion membrane due to pre-treatment.

### *3.2. Characterization studies of dye loaded Nafion membranes*

The uptake of cationic dyes by Nafion is well known, but the main aim of this work was to understand the interactions between the dyes and membrane during sorption. The UV-Vis spectra of the dye loaded samples (RhB-X and MB-X) are given in Figure 5 and these are compared with the spectrum of pure dye in the solution (given in inset).

It is seen that spectra of pure solution of RhB shows a peak maxima at 554 nm with a shoulder at 513 nm. The spectra of pure solution of MB shows two broad peaks at 613 and 662 nm, respectively. The presence of dimers in the solution for RhB [23] and MB [24] are indicated by the presence of shoulders at 513 and 613 nm, respectively. From 5 (A) it is seen that the interaction of the RhB on the three samples is quite different. The spectrum of RhB-N shows peaks at 257 and 549 nm. The peak at 257 nm corresponds to water clusters. However, in the unloaded form, sample N shows a peak at 266 nm. Thus, upon dye incorporation, it is seen that the water cluster peak has been shifted from 266 to 257 nm. This indicates that the dye loaded is present within the water cluster and is chemically bound. The peak at 549 nm corresponds to that of RhB and this is left shifted in the membrane phase as compared to the pure solution (554 nm).

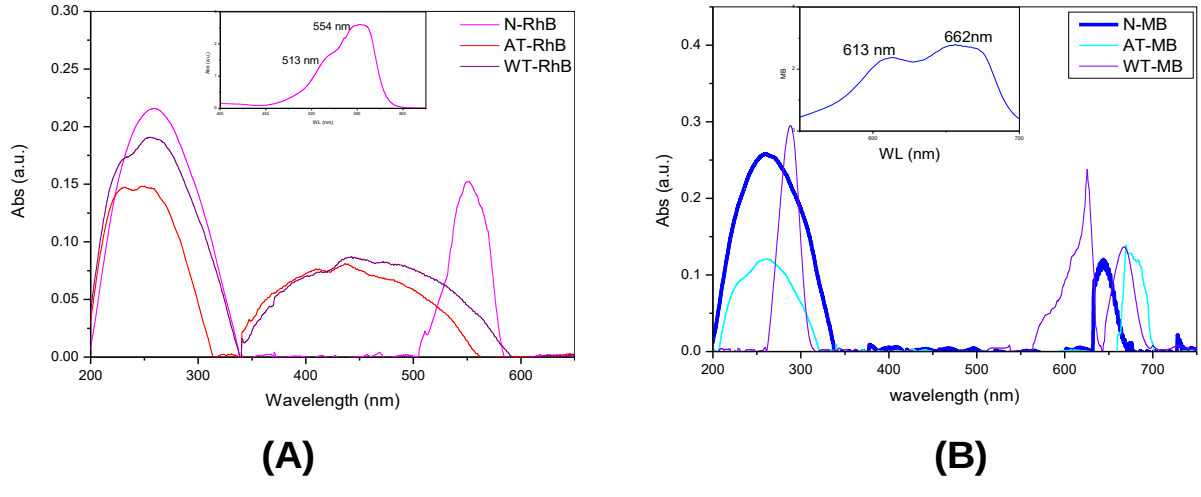


**Fig. 5.** UV visible spectra of (A) RhB and (B) MB loaded Nafion samples (Inset: Spectrum of pure dye solution).

The blue-shift could be due to the increase of electron density of azo dye as a result of the pi-pi stacking interactions of azo dye immobilized within the membrane phase. There is a small shoulder at around 511 nm. This could be attributed to the presence of dimers which exhibit a blue shift from 513 nm of pure dye. Thus, it is seen that the nature of the dye incorporated within the membrane phase is not affected. However, for sample AT and WT, interesting features are seen from the spectra. For sample AT, there are distinct peaks at 236, 253, and a very broad peak between 400 to 450 with jumps at 406 and 436 nm. The water clusters in RhB-AT show blue shift changes much more than the RhB-N sample. The main interesting feature is that the nature of RhB in AT is quite different from its pure form. The peak corresponding to the pure dye at 554 nm is not present. Moreover, the peak of the dimers is more prominent. This can be visualized as in AT, the RhB molecules within the clusters have an increased tendency to form dimers or probably give a polymeric kind of structure. The spectra of RhB incorporated WT sample shows a peak at 257 nm and a broad peak between 410 to 440 nm with a hump at 438 nm. The situation in sample WT is similar to AT but to a lesser extent. Therefore, for both AT and WT, different interactions between water-water, water-RhB and RhB-RhB molecules may occur leading to spectra completely different from sample N. Figure 5B shows the results of sorption of methylene blue by different samples. For sample N-MB, there are two peaks at 260 and 771 nm. The peak of 260 nm corresponds to that of water clusters in the presence of MB. This shows that MB interacts with the water clusters and hence a shift in the peak maximum occurs. The peak corresponding to MB is seen at 650 nm. The spectral changes indicate the interaction between MB and sample N. For AT-MB, it is seen that the peak corresponding to the water clusters is reduced in intensity. This could indicate that in the presence of MB, pure water clusters do not exist. The peak of MB is seen around 670 nm showing that there is not much change in the nature of MB in sample AT. However, it is more interesting to observe the spectrum of WT-MB. Firstly, the water cluster peak is well shifted to around 289 nm. This indicates the presence of strong interactions between the water molecules amongst each other and also with the MB molecules. The two peaks at 666 and 582 nm were correlated to that of MB and its dimer, respectively. It is seen that the dimer peak is shifted to 625 nm and there are many small humps. These suggest that in the WT sample, MB sorbed is present as both its monomeric and dimeric forms and there also exists some possibility of interactions between these forms leading to some kind of polymeric structure within the membrane phase.

The optical microscopic evaluation of N, AT and WT membranes were carried out. Preliminary studies with the bare membranes did not show any clear features. Hence, the dye incorporated membranes were analyzed and the results are shown in Figure 6. From Figure 6A, the difference in the structural features upon pre-treatment is clearly seen. Unlike sample N, both AT and WT showed lucid features. In AT, the clusters and the ionic channels were quite clear. Thus, the pre-treatment by boiling (with acid or water) leads to the opening up of the clusters and ionic channels, but the degree of opening is more with acid boiling (Sample AT). From these analyses, the area fraction occupied by the dye in each of the representative frames of N, AT and WT were calculated and represented in Figure 6B. It is observed that the fraction of area covered by the dye (RhB and MB) follows the order AT > WT > N. This indicated that upon boiling with acid or water, the opening of ionic channels results in increased sorption of dye molecules.

Thermal studies of dye incorporated Nafion membranes were carried out and compared with that of bare membranes and pure dyes. The TG and DTA plots of pure MB and MB loaded Nafion membranes are given in Figure 7. MB shows an initial water loss followed by two step decomposition in which liberation of N and Cl atoms take place in the first step followed by breakage of the C-S bonds. The exotherms at low temperature in DTA plots indicate stepwise cyclization following the liberation of N and Cl atoms.

Figure 7A1-C1 gives the TG plots of the Methylene blue incorporated Nafion membranes. For methylene blue loaded N (N-MB), the initial short wt loss step is not prominent and the final major wt loss takes place sluggishly as compared to bare N. The DTA plot also indicates the absence of the short endotherm at around 350°. The total % weight loss of N-MB is ~79% and quite similar to that of N. Membrane **AT** incorporated with MB (AT-MB) shows a weight loss of 74 % which is the same as that for bare AT (73%) and the decomposition patterns for both are similar. The DTA plot of AT-MB shows the presence of two merging endotherms at 250ºC and 350ºC, and the highest temperature endotherm is nearly at the same position as in the bare AT membrane. The thermal studies of WT incorporated with MB (WT-MB) show similar weight loss (68%) as that of WT. However, the DTA pattern of WT-MB is different from that of bare WT. The endotherm at 350ºC of WT-MB is much broader than in bare WT and the highest temperature endotherm has shifted to a much higher temperature (650 ºC) as compared to that in bare WT(550 ºC). The above TG-DTA results indicate that there is probably some bonding between the dye and Nafion involving both the side chains and the main backbone, which affects the desulfonation behaviour as well as the pattern of main PTFE backbone decomposition of the membrane. A similar type of bonding between polymer-methylene blue composites have been reported in the literature [25]. Thermal analysis of RhB loaded membranes (Figure 8) involves four decomposition steps. The initial step is associated water loss while the remaining three steps involve successive breakdown of the side chains, ether linkage and the main backbone. The corresponding DTA results show broad endotherms. Membrane N loaded with RhB (N-RhB) showed a weight loss of 86% (bare N showed 79%). The final decomposition occurs at a higher temperature compared to bare N. The DTA pattern of N-RhB is significantly different from that of bare Nafion as the endotherm at lower temperature (350 ºC) is not present and the only endotherm at higher temperature of ~ 500ºC is more sluggish than N. AT loaded with RhB (AT-RhB) showed a net weight loss of 70% and the DTA patterns of AT and AT-RhB match with each other in terms of number of endotherms and their temperature of initiation. WT loaded with RhB (WT-RhB) showed a weight loss of 64% which is much lower than the bare WT membrane. The DTA patterns showed broader endotherms at 350 ºC and 550 ºC, but unlike the WT-MB, it is seen that for WT-RhB, the highest endotherm temperature is the same as bare WT (550 ºC).

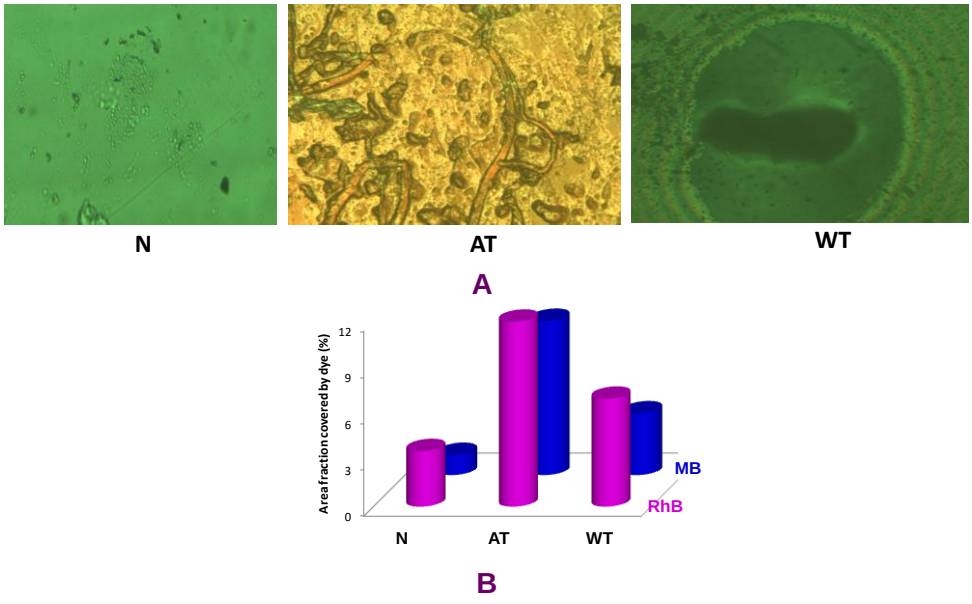


**Fig. 6.** (A) Optical microscopic images of Nafion membranes and (B) extent of dye coverage.

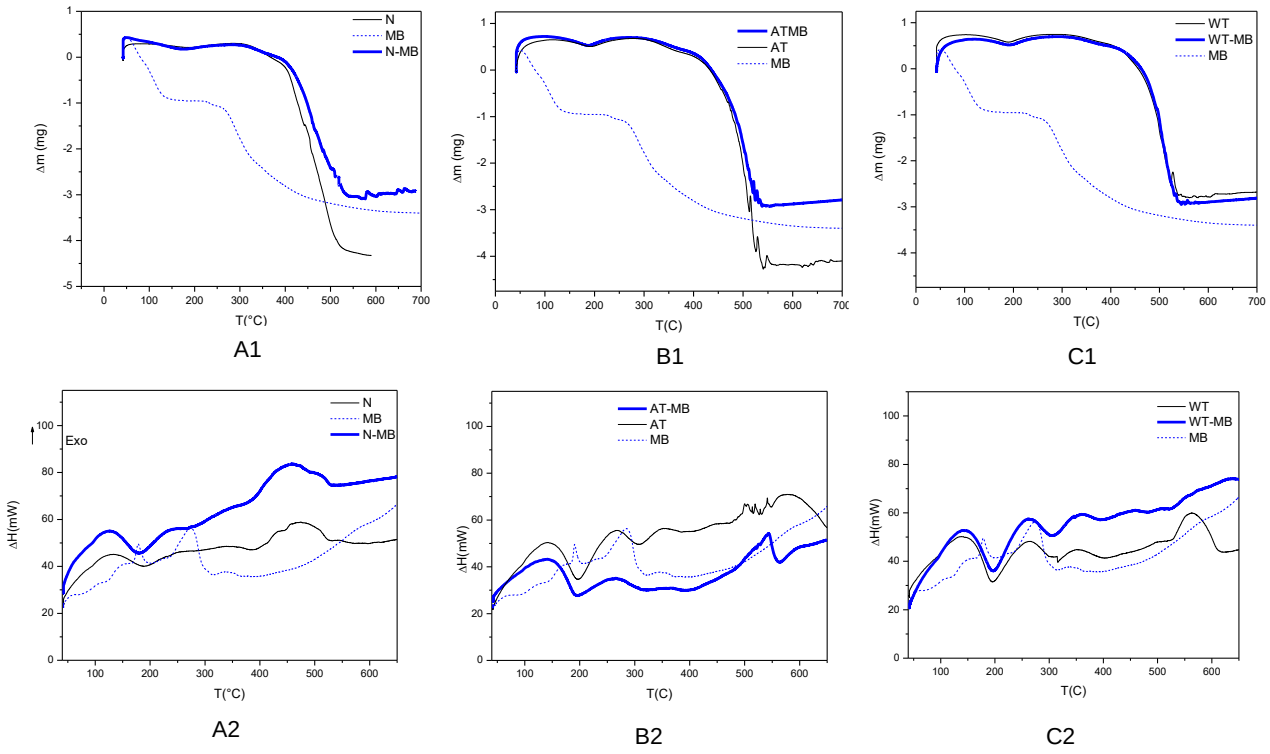


**Fig. 7.** Thermal data (A1-C1) TG and (A2-C2) DTA traces of MB loaded Nafion membranes.

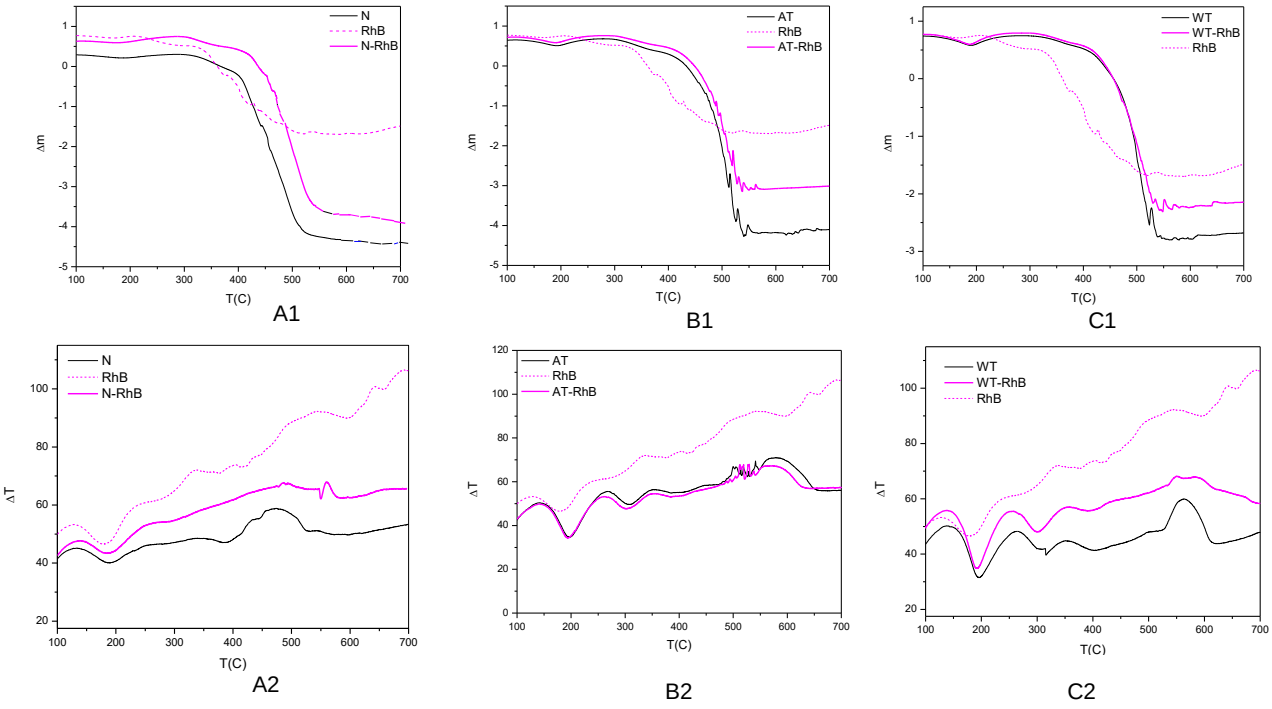


**Fig. 8.** Thermal data (A1-C1) TG and (A2-C2) DTA traces of RhB loaded Nafion membranes.

All the above results indicate that incorporation of methylene blue within Nafion membranes (N,AT,WT) shows no significant change in weight loss, but a major change in DTA patterns (peak shape, temperature ) are observed. In the case of RhB incorporated membranes, it is seen that there is a significant decrease in the total weight loss depending on the pre-treatment of Nafion and also changes in DTA patterns. It is also interesting to note that without any pre-treatment, the TG patterns resemble that of pure N irrespective of the incorporated dye. This indicates that in dye loaded N membranes, the thermal decomposition of the dyes get arrested. This could probably indicate that since the structure is not open, the dyes are just exchanged and not present within the clusters and channels. These studies give an insight that although both the dyes are cationic in nature, the interaction with Nafion membranes (pre-treated differently) is different.

### *3.3. Permeation studies of dyes using pre-treated Nafion membranes*

Permeation of dye samples through Nafion samples were carried out to gain an insight of various processes in the membranes and the effect of pre-

treatment on the membrane transport process. Since Nafion is a cation exchange membrane, it was thought that the pH of the external solution would affect the affinity of the membrane towards different cations. However, a high degree of selectivity in the uptake cannot be achieved by controlling only the pH. Earlier studies indicated that dye uptake by various sorbents could be carried out at a pH of 4-6 [26]. This was due to the competition of $H^+$ at lower pHs for the sorption sites and at higher pHs, hydrolysis of dyes occur, thus reducing the amount of dye present in its cationic form. Moreover, it is reported that a change in pH of the solution results in the formation of different ionic species (Figure 9).

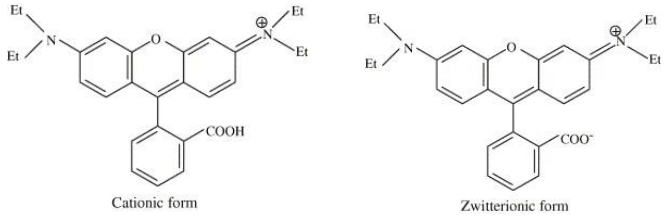


**Fig. 9.** Molecular species of RhB.

At pH values lower than 2, the aggregation of RhB is known to occur [26]. Up to a pH of 4, the RB ions have a cationic and monomeric molecular form. Thus, RB ions can enter into the pore structure. At a pH value higher than 4, the zwitterionic form of RB in water may increase the aggregation of RB to form a bigger molecular form (dimer) and become unable to enter into the pore. Ghanadzadeh *et al.* [27] have studied the aggregation of RhB in the microporous solid hosts. Lopez Arbeloa *et al.* [28] determined the equilibrium constant for the dimer⇔monomer transition of RhB in aqueous solution. The greater aggregation of the zwitterionic form is due to the attractive electrostatic interactions between the carboxyl and xanthene groups of monomers. At a pH value higher than 8, the preponderance of $OH^-$ generates a competition between –N+ and $–COO^-$ and will decrease the aggregation of RB, which causes an increase in the adsorption of RB ions on the carbon surface. Hence, the permeation studies were carried out at pH of 6. The permeation was carried out using the membranes pre-treated differently in $H^+$ forms.

The concentration profiles for the transport of the cationic dyes (Rhodamine B (RhB) and methylene blue (MB)) through Nafion in H+ form are given in Figures 10A and 10B, respectively. Interesting features are observed from the plots. It is seen that the net amount of RhB permeated (Figure 10A) is more than MB (Figure 10B) for all the three different types of membranes. However, it is to be mentioned that saturation in the concentration profiles were seen at an earlier time period for MB (~4h) as compared to RhB (~6h). This can be explained as follows. The permeation is a combination of both the sorption and desorption process. Therefore, it is thought that the RhB molecules within the membrane may not be desorbed with the same rate and therefore the saturation occurs at a later time period. This is possible due to the enhanced interaction between dye molecules amongst each other and also within the membrane sites, thus making desorption slower than that of MB.

The permeation flux of the solute across a membrane thickness (δ) can be correlated [29, 30] to changes in the concentration in the membrane phase and also to changes in the solute concentration $C_R$ in a known volume of the receiving phase $V_R$ upon permeation through an available area A and represented by Eqs. 4 and 5.

$$J = D*(C_{FM} - C_{RM}) \Big/ \delta \tag{4}$$

$$J = \left(\frac{V_R}{A}\right) * \left(\frac{\delta C_R}{\delta t}\right) \tag{5}$$

Thus by combining Eqs. 4 and 5, the value of D can be calculated as follows:

$$\left(\frac{V_R}{A}\right) * \left(\frac{\delta C_R}{\delta t}\right) * \frac{\delta}{(C_{FM} - C_{RM})} = D \tag{6}$$

In the present study, the membrane thickness and area of permeation are 0.01778 cm and 0.79 $cm^2$, respectively and the volume of receiving solution ($V_R$) was 10 mL. The slope of the plot of amount permeated with time (Fig. 10) can give the concentration variation with time. The permeability coefficient in the feed phase is given by Eq. 7, wherein P is the permeability coefficient (cm/s), $C_o$ and C the concentration of dye initially and at time t in feed phase, A effective membrane area ($cm^2$), ε the membrane porosity, V ($cm^3$) volume of the feed phase and t is the elapsed time. The porosity is given by Eq. 8, where A and δ are area and thickness of the membrane and ρ the density of water.

$$\ln\frac{C}{C_o} = -\varepsilon * P * t * \frac{A}{V_F} \tag{7}$$

$$\varepsilon = \frac{\text{water content}}{A * \delta * \rho} \tag{8}$$

Hence, the treatment of permeation data was carried out using the different equations and diffusion and permeability coefficients were calculated and given in Table 3.

**Table 3**
Diffusion (D) and Permeability (P) coefficients for RhB and MB using different pretreated membranes in $H^+$ form.

| Memb. | Rhodamine B | | Methylene Blue | |
|---|---|---|---|---|
| | D x $10^5$ ($cm^2$/s) | P x $10^3$ (cm/s) | D x $10^5$ ($cm^2$/s) | P x $10^3$ (cm/s) |
| N | 0.29 | 0.52 | 0.704 | 0.49 |
| AT | 4.9 | 3.1 | 5.9 | 3.9 |
| WT | 2.2 | 1.7 | 5 | 3.0 |

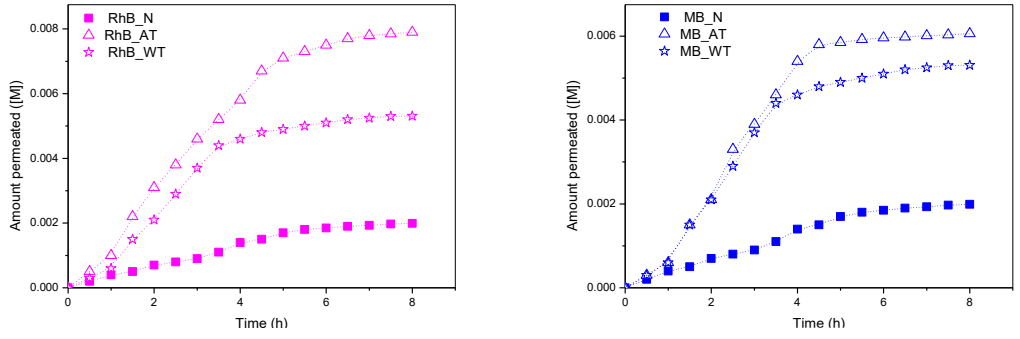


(A) (B)

**Fig. 10.** Permeation studies of (A) Rhodamine B and (B) Methylene Blue.

From Table 3, it is seen that the values of P are 100 orders more than that of D and the order followed by both D and P is AT > WT > N for the three different pre-treated Nafion membranes. Thus, it is very clear that the pre-treatment has an effect on the permeation parameters. This can be understood from the fact that upon pre-treatment with acid, an open structure is generated (as seen from microscopic studies) and therefore the diffusion of molecules within the membrane structure and the overall permeation becomes more favourable as compared to the untreated membranes. It is also seen that when P is large, solutes will diffuse rapidly across a membrane under a given concentration gradient. It is understood that P symbolizes several factors: partitioning between the solution and membrane, membrane thickness and diffusion coefficient of the solute in the membrane. It is observed from Table 3 that P is more for MB as compared to RhB. This can be understood as follows. MB is a smaller ion as compared to RhB. The steric hindrance is caused due to the bulky 3D structure of RhB leading to its lower P values. Thus, it is clear that permeation of dyes not only depends upon the cation exchange property of Nafion but also its structural changes due to pre-treatment, which affects the overall permeation.

## 4. Conclusions

Nafion membrane was subjected to different pre-treatment procedures prior to its use. UV-Visible spectroscopic analysis of these different samples showed that pre-treatment with acid under boiling conditions leads to the presence of more water clusters within the membrane. Thermal studies showed that pre-treatment also affects the rigidity of the PTFE backbone. UV-Visible spectroscopic analysis of dye loaded membranes indicate that the dye is present within the water clusters and the formation of dimers occurs. Optical microscopic evaluation of dye loaded N, AT and WT samples revealed a clear difference in structural features as a result of pre-treatment. Thus, the pre-treatment by boiling with acid or water leads to the opening up of the clusters and ionic channels. Thermal studies establish the presence of bonding between the dye and Nafion involving both the side chains and the main backbone. These studies give an insight that though both the dyes are cationic in nature, the interaction with Nafion membranes (pre-treated differently) is different. Permeation studies reveal that the bulky nature of rhodamine dye results in its low permeability coefficient. Thus, it is clear that permeation of dyes depend both on the nature of dye as well as the structural changes within the membrane structure due to pre-treatment.

Permeation of cationic dyes like Rhodamine B and methylene blue were carried out. Dye permeation through the uptake of cationic dyes like Rhodamine B and methylene blue occurs via a cation exchange process. This is dependent on the nature of the dye. However, the permeation of the dyes across the membranes depends on the structural aspects of the membranes. The pre-treatment procedure has a marked effect on the structure of the membranes, as ascertained by various techniques. Characterization studies also confirm the presence of dimeric forms of the dye within the membrane surface. The changes in structure due to pre-treatment results in a change in the diffusion flux across the membrane.

## Acknowledgements

The authors would like to thank Dr. P. D. Naik, AD Chemistry Group and Head ACD, BARC for his constant support.

## References

[1] J. Ramkumar, Nafion Perfluorosulphonate Membrane: Unique Properties and Various Applications, Chapter 13, in: Functional Materials, Banerjee, Tyagi (Eds), Elsevier, pp. 549-577.

[2] A.Vishnyakov, A.V. Neimark, Molecular dynamics simulation of microstructure and molecular mobilities in swollen Nafion membranes, J. Phys. Chem. B 105 (2001) 9586–9594.

[3] F. Xu, S. Leclerc, D. Stemmelen, J.-C. Perrin, A. Retournard, D. Canet, Study of electro-osmotic drag coefficients in Nafion membrane in acid, sodium and potassium forms by electrophoresis NMR, J. Membr. Sci. 536 (2017) 116-122.

[4] Q.L. Liu, S. Lotze, H.J. Bakker, Vibrational and structural relaxation of hydrated protons in Nafion membranes, Chem. Phys. Lett. 670 (2017) 102-108.

[5] Q. Duan, H. Wang, J. Benziger, Transport of liquid water through Nafion membranes, J. Membr. Sci. 392–393 (2012) 88–94.

[6] J. Ramkumar, E.K. Unnikrishnan, B. Maiti, P.K. Mathur, Facilitated transport of halides through Nafion ionomer membrane modified with lanthanide complexes, J. Memb. Sci. 141 (1998) 283-288.

[7] J. Ramkumar, B. Maiti, T.S. Krishnamoorthy, Transport of some nitrogen heterocyclic and aromatic compounds through metal ion containing Nafion ionomer membrane, J. Membr. Sci. 125 (1997) 269-274.

[8] J. Ramkumar, K.S. Shrimal, B. Maiti, T.S. Krishnamoorthy, Selective permeation of $Cu^{2+}$ and $UO_2^{2+}$ through a Nafion ionomer membrane, J. Membr. Sci. 116 (1996) 31-37.

[9] J. Ramkumar, S. Chandramouleeswarana, Metal ion uptake behaviour of Nafion in presence of organic complexing reagents, MOJ Bioorg. Org. Chem. 1 (2017) 1-3.

[10] J. Ramkumar, T. Mukherjee, Role of ion exchange in permeation processes, Talanta 71 (2007) 1054-1060.

[11] J. Ramkumar, T. Mukherjee, Effect of aging on the water sorption and ion exchange studies on Nafion and Dowex resins: Transition metal ions-proton exchange systems, Sep. Purif. Technol. 54 (2007) 61-70.

[12] J. Ramkumar, B. Venkataramani, Alkali metal ion – proton exchange equilibria and water sorption studies on Nafion 117 membrane and Dowex 50 W resins: Effect of long storage or aging, BARC / 2004 / E /026.

[13] Y. Fan, D. Tongren, C.J. Cornelius, The role of a metal ion within Nafion upon its physical and gas transport properties, Eur. Polym. J. 50 (2014) 271-278.

[14] D.K. Kim, E.J. Choi, H.H. Song, M.S. Kim, Experimental and numerical study on the water transport behavior through Nafion® 117 for polymer electrolyte membrane fuel cell, J. Memb. Sci. 497 (2016) 194-208.

[15] M. Basu, J. Ramkumar, Understanding the structural changes in Nafion due to shelf-life and pre-treatment: Thermo dynamical approach of water and metal ion sorption, Ind. J. Adv. Chem. Sci. 3 (2014) 19-24.

[16] J. Kabrane, A.J. A. Aquino, Electronic structure and vibrational mode study of Nafion membrane interfacial water interactions. J. Phys. Chem. A 119 (2015) 1754-1764.

[17] L. Liu, S. Lotze, H.J. Bakker, Vibrational and structural relaxation of hydrated protons in Nafion membranes, Chem. Phys. Lett. 670 (2017) 102-108.

[18] A. Vishnyakov, A.V. Neimark, Self-assembly in Nafion membranes upon hydration: Water mobility and adsorption isotherms, J. Phys. Chem. B 118 (2014) 11353-11364.

[19] W. Chen, F. Cui, L. Liu, Y. Li, Assembled structures of perfluorosulfonic acid ionomers investigated by anisotropic modeling and simulations, J. Phys. Chem. B 121 (2017) 9718-9724.

[20] M. Turhan, S. Sayar, S. Gunasekaran, Application of Peleg model to study water absorption in chickpea during soaking, J. Food Eng. 53 (2002) 153–159.

[21] S.H. deAlmeida, Y. Kawano, Ultraviolet-visible spectra of Nafion membrane, Eur. Polym. J. 33 (1997) 1307-1311.

[22] S.H. deAlmeida, Y. Kawano, Thermal behavior of Nafion membranes, J. Therm. Anal. Cal. 58 (1999) 569-577.

[23] T. Kajiwara, R.W. Chambers, D.R. Kearns, Dimer spectra of Rhodamine B, Chem. Phys. Lett. 22 (1973) 37-40.

[24] R. Sanan, T.S. Kang, R.K. Mahajan, Complexation, dimerisation and solubilisation of methylene blue in the presence of biamphiphilic ionic liquids: a detailed spectroscopic and electrochemical study, Phys. Chem. Chem. Phys. 16 (2014) 5667-5677.

[25] P.R. Somani, R. Marimuthu, A.K. Vishwanath, S. Radhakrishnan, Thermal degradation properties of solid polymer electrolyte (poly(vinyl alcohol)+phosphoric acid)/methylene blue composites, Poly. Deg. Stab. 79 (2003) 77-83.

[26] J. Ramkumar, S. Chandramouleeswaran, V. Sudarsan, R.K. Mishra, C.P. Kaushik, K. Raj, A.K. Tyagi, Barium borosilicate glass as a matrix for the uptake of dyes, J. Hazard. Mater. 172 (2009) 457-464.

[27] A. Ghanadzadeh, M.A. Zanjanchi, Self-association of Rhodamine dyes in different host materials, Spectrochem. Acta A Mol. Biomol. Spec. 57 (2001) 1865-1871.

[28] F.L. Arbeloa, P.R. Ojeda, I.L. Arbeloa, Dimerization and trimerization of rhodamine in aqueous solution. Effect on the fluorescence quantum yield, J. Chem. Soc. Faraday Trans. 2 (1988) 1903-1912.

[29] N. Lakshminarayaniah, Transport phenomena in membranes, Academic Press, New York, 1969.

[30] M.S. Kang, K.S. Yoo, S.J. Oh, S.H. Moon, A lumped parameter model to predict hydrochloric acid recovery in diffusion dialysis, J. Membr. Sci. 188 (2001) 61-70.